Throughput limitations for the direct space-to-time pulse shaper

S. Costantino and O. E. Martínez

Laboratorio de Electrónica Cuántica, Departamento de Física, Universidad de Buenos Aires, Pabellón 1, Ciudad Universitaria, 1428 Buenos Aires, Argentina

Received November 15, 2000; revised manuscript received March 12, 2001

Analytical expressions for the throughput of a direct space-to-time encoder are used to determine possible output distortions and limitations. The interplay of relevant design parameters is analyzed to avoid such distortions and optimize the performance of the encoder. It is proved that the different propagation angles of the beams in the system produce drastic variations in the coupling coefficient to an optical fiber. It is also shown that it is possible to solve this problem when the throughput of the system is reduced. © 2001 Optical Society of America

OCIS codes: 060.2330, 060.4510, 320.7160, 320.5540.

1. INTRODUCTION

Progress in optical communications continually demands faster methods for information transmission. In this context, Leaird and Weiner[1] have recently introduced the so-called direct space-to-time (DST) pulse encoding based on the picosecond pulse shaper reported in some previous papers.[2,3]

The system shows similarities to a conventional Fourier-transform pulse shaper. The method basically consists in pixelating an input femtosecond pulsed laser beam so that each pixel can be independently modulated. Light is then dispersed by a grating followed by a Fourier filter, consisting of a lens and a slit positioned at the focal plane. As a result, each pixel beam arrives at the slit with a time delay proportional to the pixel number, and hence the spatial information of the array of pulses is linearly converted into time information. This last part of the system is described in Fig. 1.

In this paper we compute an analytical expression for the electric field of the array of pulses that propagate from the grating to the slit. Such expression is used to determine the throughput of the DST as a function of design parameters. The result shows that power after the slit goes as Leaird and Weiner[1] predicted only under certain particular conditions. Moreover, when the information is coupled into an optical fiber, we show that drastic limitations appear, yielding a rapidly decaying throughput as the number of pixels increases.

To acquire some physical insight of the system, we chose five parameters so that their interplay would describe the behavior of the DST under different conditions. Two of these relevant magnitudes are pixel size at the grating (σ) and the distance from the mth pixel to the center of the array (h_m). The astigmatic parameter, the wavelength, and the focal length of the lens will define the third parameter that is the pixel spot size at the slit plane (R), depicted in Fig. 2. The fourth magnitude is the spatial dispersion of the input beam spectrum at the slit plane (S) that is determined by the dispersion of the grating, the focal length, and the limited bandwidth of the laser pulse (Fig. 3). The last parameter is the slit aperture, and these five parameters are enough to describe the system qualitatively.

The first relevant consideration is that, after the slit plane, the different pixel beams will propagate in different directions; and, to have a superposition, the diffraction angle that is due to the slit must be bigger than the propagation angle. This relation imposes the first limitation to the size of the aperture (D) and carries a decrease in the throughput. Furthermore, the more pixels we want, the smaller the aperture must be. On the other hand, to increase the throughput, D should be bigger that R so that the spot is not blocked by the slit.

The design of the DST should also consider that, if S were bigger than the slit aperture, it would give rise to pulse broadening and throughput loss. Apart from that, if S were larger than R, then the different frequency components of the pulse would not overlap in the slit; but a smaller bandwidth would imply that the input pulse is broader than the intended pixel duration.

In this paper we obtain design equations that adequately describe the interplay of these parameters to optimize the performance of the system.

2. ANALYTICAL DESCRIPTION

To achieve an analytical solution for the throughput, the pixels are assumed to have Gaussian profiles. This approximation is not severe; even if no apodization is used, high spatial frequencies will typically be lost because of diffraction and the profile will be smoothed upon propagation. Similar arguments hold for the Gaussian approximation used for the slit transmission.

For our calculations we follow the formalism presented in Refs. 4 and 5 and the notation therein that is slightly different from that used by Leaird and Weiner.[1] As depicted in Fig. 1, the incidence angle is γ and the output

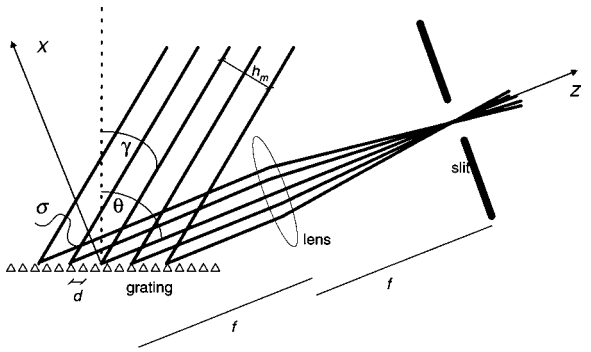

Fig. 1. Schematic of the space-to-time shaper. Five pixels of width σ are represented.

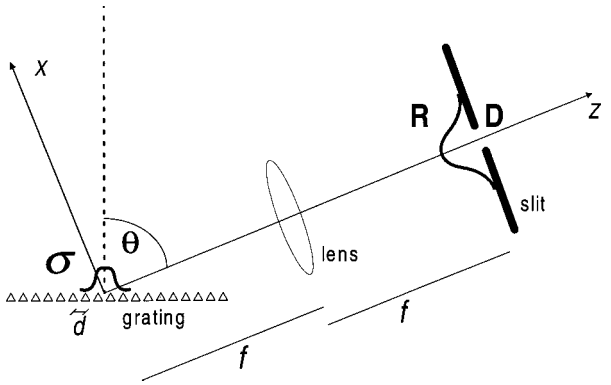

Fig. 2. Pixel spot size at the grating is σ, and it becomes R at the slit plane. D is the aperture of the slit.

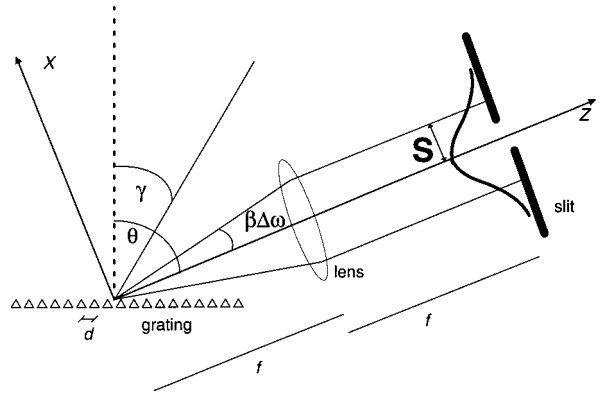

Fig. 3. Limited bandwidth of the laser pulse $\Delta\omega$, the dispersion of the grating β, and the focal length of lens f determine the spatial dispersion of the input beam spectrum at the slit plane S.

angle is θ. The wavelength of the central frequency is λ. The astigmatic parameter α and the dispersion β are given by

$$\alpha = -\frac{\cos(\gamma)}{\cos(\theta)}, \tag{1}$$

$$\beta = \frac{\lambda^2}{2\pi c d \cos(\theta)}, \tag{2}$$

where c is the speed of light and d is the groove spacing.

The input beam amplitude of any pixel of the array that is reflected on the grating is given by

$$a_g(x, \omega) = a \exp\left(-\frac{\omega^2}{2\Delta\omega^2}\right) \exp\left[-ik\frac{(x - h_m)^2}{2q}\right], \tag{3}$$

where a is the electric field amplitude, ω is the central frequency of the pulse, $\Delta\omega$ is the bandwidth, $k = \omega/c$ is the wave number in vacuum, x is the lateral dispersion coordinate, and h_m is the distance from pixel m to the center of the array. q is defined by

$$\frac{1}{q} = \frac{n}{\rho} - i\frac{2}{k\sigma^2}, \tag{4}$$

where ρ is the phase front radius of curvature, n is the diffraction index, and σ is the spot radius at the beam waist. We obtain the expression for the pulse at the focal plane using the matrix formalism presented by Martínez.[5] As a result, the amplitude of the electric field is given by the expression

$$\begin{aligned} a_{\text{focus}}(x, \omega) = a &\exp\left(-\frac{\omega^2}{2\Delta\omega^2}\right) \exp\left(-ik\frac{\beta\omega h_m}{\alpha}\right) \\ &\times \exp\left[-\frac{k^2\sigma^2}{4f^2\alpha^2}(x - f\beta\omega)^2\right] \\ &\times \exp\left(-ik\frac{h_m x}{f\alpha}\right), \end{aligned} \tag{5}$$

where f is the focal distance of the lens, assuming that q is pure imaginary, which mens that the beam waist is located at the grating ($z = 0$) for the central pixel.

Field amplitude in Eq. (5) has four exponential terms. The first one shows the pulse's limited bandwidth. The second one represents the time delay between the central pixel and one at a distance h_m, and it provides the space-to-time scaling constant $\beta k/\alpha$. The third term is related to the Gaussian spatial profile at the focal plane and shows that the slit can be slightly moved without altering the temporal output as stated by Leaird and Weiner[6] The last one appears because of the different propagation angle for each pixel beam.

We achieve the normalized intensity of the beam after the slit by multiplying Eq. (5) by the slit transmission function T_{slit}, where D represents the size of the aperture:

$$T_{\text{slit}} = \exp\left(-\frac{x^2}{2D^2}\right). \tag{6}$$

The integration of the normalized intensity yields the DST throughput T:

$$T = \left[1 + \frac{f^2(2\alpha^2 + k^2\beta^2\Delta\omega^2\sigma^2)}{2D^2k^2\sigma^2}\right]^{-1/2}. \tag{7}$$

3. THROUGHPUT ANALYSIS

It is possible to analyze the throughput given in Eq. (7) in terms of the parameters presented in Section 1. Pixel spot size at the slit plane R and spatial dispersion of the input beam spectrum S can be precisely described by

$$R = \frac{|\alpha| f}{\sqrt{2} k \sigma}, \tag{8}$$

$$S = \beta \Delta \omega f. \tag{9}$$

The result can be expressed as a function of two dimensionless parameters R/D and S/R:

$$T = \left[1 + \frac{R^2}{2D^2} \left(1 + \frac{S^2}{R^2} \right) \right]^{-1/2}. \tag{10}$$

The parameter S/R is related to the ratio of the pixel time duration and the input pulse width. This can be seen in relation (11), where the first factor is proportional to the inverse of the input pulse time duration and the second one is the space-to-time scaling constant times the pixel spot size at the grating:

$$\frac{S}{R} \propto \Delta \omega \frac{\beta k \sigma}{|\alpha|}. \tag{11}$$

Equation (10) is plotted in Fig. 4 as a function of S/R, with the ratio of the pixel spot size and the slit aperture (R/D) as a parameter. This shows that only for large S/R the throughput scales as the ratio of the input pulse width and the temporal window generated by the array of pixels (R/S) as quoted in Ref. 1. This is shown in Fig. 4 where the slope of the throughput asymptote is parallel to R/S.

The asymptotic value of the throughput is D/R and is of the order of the inverse number of pixels for small S/R, but $S/R < 1$ implies that the input pulse duration is larger than the pixel time duration, which is not a physically interesting condition. The pixel spot size σ can be small, but the pixel time duration will not be shorter than the input pulse.

To avoid time pattern distortions, the diffraction angle corresponding to the slit aperture should be bigger than the one at which each pixel beam propagates:

$$\frac{f\alpha}{h_m} < Dk. \tag{12}$$

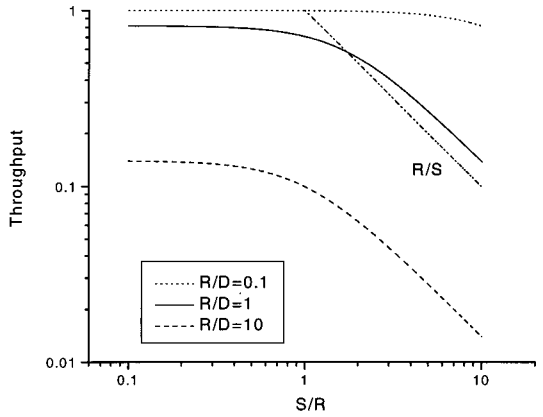

Fig. 4. Throughput of the DST shaper as a function of the ratio of pixel time duration and input pulse width (S/R). The ratio of the pixel beam at the slit plane and the aperture (R/D) is an upper bound to the number of pixels. For large S/R, the throughput scales as the ratio of the input pulse width and the temporal window generated by the array of pixels (R/S).

This condition yields a restriction on the number of pixels, replacing the distance from the center of the array to the mth pixel (h_m) by $m\xi\sigma$, where the design parameter ξ defines the ratio of pixel separation and pixel width:

$$\frac{R}{D} > m\xi. \tag{13}$$

To have a better idea of the throughput characteristics that can be achieved in realistic conditions, we now present some numerical examples. The first situation we consider is similar to the one stated in Ref. 1 where the authors have a 150-fs pulse from a titanium:sapphire laser, centered at 850 nm. The incidence angle is $\gamma = 47°$ and the diffraction angle $\theta = 53°$, the grating has 1800 lines mm, the pixel spot size is 20 μm, and they are separated by 60 μm. For a 100-mm focal-length lens and a 100-μm slit, the throughput calculation results in 2%. Another possible setup consists in a 100-fs pulse centered at 800 nm, with a 1200-line/mm diffraction grating at normal incidence. The focal length of the lens is $f = 100$ mm, the pixel spot size is 50 μm and $\xi = 3$, the slit aperture is 100 μm, and the throughput becomes 1.5%.

4. OPTICAL FIBER COUPLING

A different situation is encountered if, instead of a slit, the beam is coupled into an optical fiber. Here, we proceed in a similar manner as above to compute the coupling coefficient of the DST to a monomode optical fiber. We describe the electric field at the focal plane (5) as a linear combination of the fiber modes and calculate the different coefficients.

In this case the only mode of the fiber was assumed to have the form[7]

$$\Psi_{01} = \frac{1}{\sqrt{\pi} D} \exp\left[-\frac{(x^2 + y^2)}{2D^2} \right], \tag{14}$$

and we achieved the coupling coefficient a_{01} using the following procedure stated in Ref. 8:

$$a_{01} = \int_{-\infty}^{\infty} \Psi_{01}(x, y) E(x, y) \mathrm{d}x \mathrm{d}y, \tag{15}$$

where $E(x, y)$ is normalized to a unit area.

As a result, we obtained a function whose square modulus can be integrated in frequency to achieve the throughput in this new situation:

$$T = \frac{4R_y \exp\left[-2 \dfrac{m^2 \xi^2}{\left(1 + \dfrac{R^2}{D^2} \right)} \right]}{\left(1 + \dfrac{D^2}{R^2} \right)^{1/2} \left(1 + \dfrac{D^2}{R^2} + \dfrac{S^2}{R^2} \right)^{1/2} \left(1 + \dfrac{R_y^2}{D^2} \right) R}, \tag{16}$$

where R_y is the pixel spot size in the direction perpendicular to the dispersion plane.

Equation (16) is plotted in Fig. 5 as a function of S/R. R_y was chosen to maximize the throughput.

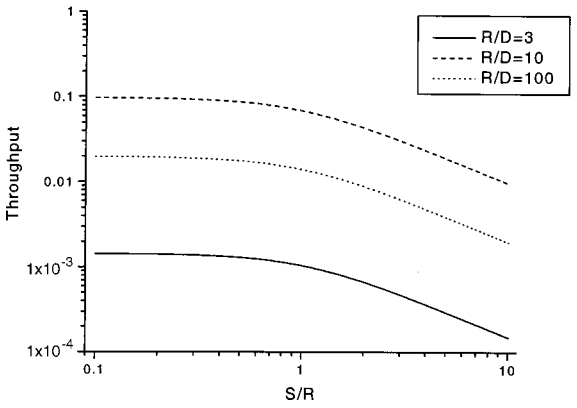

Fig. 5. Coupling efficiency to a monomode optical fiber of the DST as a function of the ratio of pixel time duration and input pulse width (S/R) for the fourth pixel and $\xi = 1.5$.

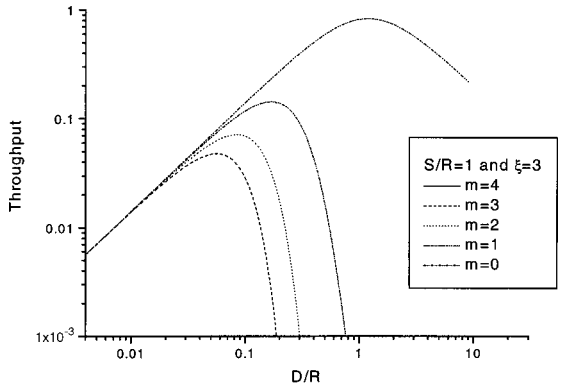

Fig. 6. Coupling coefficient to a monomode optical fiber as a function of D/R for different pixels and $S/R = 1$. When we reduce D/R, the throughput decreases and the intensities of the pixels become balanced.

In Fig. 6 the throughput for different pixels is plotted for a fixed S/R condition as a function of D/R. It becomes clear that the throughput for each pixel is different and that it drastically decreases for pixels that are more distant from the center of the array. To avoid this power difference between pixels, the ratio D/R must be properly designed. For a large number of bits to transmit, the pixel spot size at the fiber plane should be much larger than the fiber core, and consequently the throughput will decrease. This effect is due to the sensitivity of the fiber coupling efficiency to the angle of incidence. High-order pixels will come at angles larger than the acceptance angle of the fiber.

If we consider the first case described in the numerical examples, when we replace the slit for a 6-μm core single-mode fiber, the coupling coefficient for the tenth pixel becomes 0.16%. For the second case (normal incidence), with the same fiber, the throughput is 0.13%.

It is possible to calculate the design parameter D/R that satisfies that the ratio of the throughput of the mth pixel and the central pixel is larger than a fixed constant $\exp(-\eta)$:

$$\eta > \frac{2m^2\xi^2\dfrac{D^2}{R^2}}{1+\dfrac{D^2}{R^2}}. \tag{17}$$

When we use inequality (17) it is easy to see that, for $D/R \ll 1$, the number of pixels that have similar intensities is proportional to R/D. So when we require that the intensities of the pulses do not vary more than 10%, in the situation described in the first example, it is possible to send 110 bits through an optical fiber by use of the DST.

Furthermore, assuming the conditions $R \approx S$ and $D/R \ll 1$, we obtain a formula for the throughput that considers only the number of pixels that we want to send and the tolerance to power variations.

$$T < \frac{2\sqrt{\eta}\exp(-\eta)}{N\xi}, \tag{18}$$

where N represents the total number of pixels.

5. CONCLUSIONS

In conclusion, the analytical expression for the throughput in terms of design parameters allows us to describe the behavior of the pulse shaper precisely. We have shown that the different propagation angles of the beams in the DST produce huge variations in the coupling coefficient to an optical fiber and that this can be solved when we reduce the size of the aperture, hence decreasing the throughput. This effect was not evident when we used a slit, because all the power could go through the slit for any propagation direction. Therefore we have obtained useful expressions to calculate the throughput as a function of the number of pixels and the tolerance to intensity difference between them.

REFERENCES

1. D. E. Leaird and A. M. Weiner, "Femtosecond optical packet generation by a direct space-to-time pulse shaper," Opt. Lett. **24**, 853–855 (1999).
2. C. Froehly, B. Colombeau, and M. Vampouille, "Shaping and analysis of picosecond light pulses," in *Progress in Optics*, E. Wolf, ed. (North-Holland, Amsterdam, 1983), Vol. 20, p. 63.
3. Ph. Emplit, J.-P. Hamaide, and F. Reynaud, "Passive amplitude and phase picosecond pulse shaping," Opt. Lett. **17**, 1358–1360 (1992).
4. O. E. Martínez, "Gating and prism compressors in the case of finite beam size," J. Opt. Soc. Am. B **3**, 929–934 (1986).
5. O. E. Martínez, "Matrix formalism for pulse compressors," IEEE J. Quantum Electron. **QE-24**, 2530–2536 (1988).
6. D. E. Leaird and A. M. Weiner, "Chirp control in the direct space-to-time pulse shaper," Opt. Lett. **25**, 850–852 (2000).
7. D. Marcuse, "Gaussian approximation of the fundamental modes of the graded-index fibers," J. Opt. Soc. Am. **68**, 103–109 (1978).
8. A. B. Buckman, *Guided-Wave Photonics* (Saunders, Philadelphia, Pa., 1992), p. 150.